

This document is confidential and is proprietary to the American Chemical Society and its authors. Do not copy or disclose without written permission. If you have received this item in error, notify the sender and delete all copies.

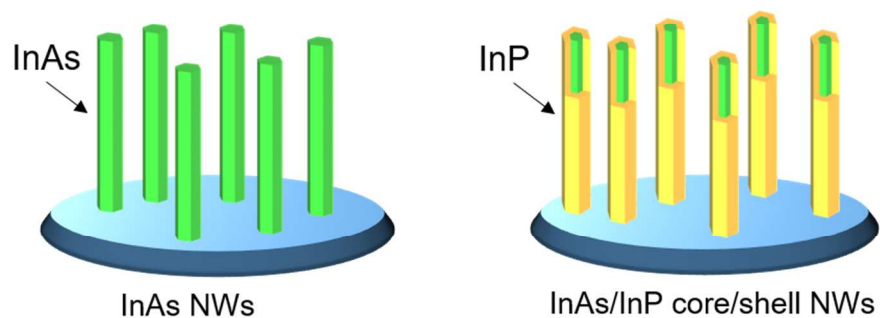
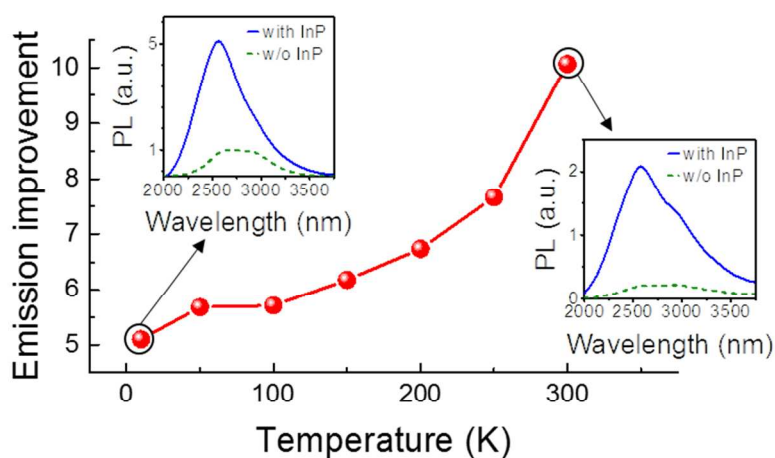
### Ten-fold Enhancement of InAs Nanowire Photoluminescence Emission with an InP Passivation Layer

Journal:	<i>Nano Letters</i>
Manuscript ID	nl-2017-00803t.R1
Manuscript Type:	Communication
Date Submitted by the Author:	02-May-2017
Complete List of Authors:	Jurczak, Pamela; University College London, Electronic and Electrical Engineering Zhang, Yunyan; University College London, ee Wu, Jiang; University College London, Electronic and Electrical Engineering Sanchez, Ana M.; University of Warwick, Department of Physics Aagesen, Martin ; University of Copenhagen, Center for Quantum Devices, Niels Bohr Institute Liu, Huiyun; University College London, Department of Electronic and Electrical Engineering

SCHOLARONE™  
Manuscripts

# Ten-fold Enhancement of InAs Nanowire Photoluminescence Emission with an InP Passivation Layer

## Table of Content



# Ten-fold Enhancement of InAs Nanowire Photoluminescence Emission with an InP Passivation Layer

*Pamela Jurczak,\*<sup>†□</sup> Yunyan Zhang,\*<sup>†□</sup> Jiang Wu,\*<sup>†</sup> Ana M. Sanchez,<sup>‡</sup> Martin Aagesen,<sup>#</sup> and Huiyun Liu<sup>†</sup>*

<sup>†</sup>Department of Electronic and Electrical Engineering, University College London, London WC1E 7JE, United Kingdom

<sup>‡</sup>Department of Physics, University of Warwick, Coventry CV4 7AL, United Kingdom

<sup>#</sup>Center for Quantum Devices, Niels Bohr Institute, University of Copenhagen, Universitetsparken 5, 2100 Copenhagen, Denmark

**ABSTRACT:** In this letter, we demonstrate that a significant improvement of optical performance of InAs nanowires can be achieved by capping the core InAs nanowires with a thin InP shell, which successfully passivates the surface states reducing the rate of non-radiative recombination. The improvements have been confirmed by detailed photoluminescence measurements, which showed up to ten-fold increase in the intensity of room-temperature photoluminescence from the capped InAs/InP nanowires compared to the sample with core-only InAs nanowires. Moreover, the nanowires exhibit high stability of total photoluminescence emission strength across temperature range from 10 to 300 K as a result of strong quantum confinement. These findings could be the key to successful implementation of InAs nanowires into optoelectronic devices.

**KEYWORDS:** Nanowires, InAs, self-catalyzed, photoluminescence

1  
2  
3  
4  
5  
6 InAs is considered to be one of the most suitable semiconductors for mid-wave infrared (mid-IR)  
7  
8 devices such as lasers or detectors due to its narrow, direct bandgap and high electron mobility.<sup>1</sup>  
9  
10 Combination of these material properties and unique 1D structure of nanowires (NWs) enables  
11  
12 creation of a new generation of nanoscale photonic and optoelectronic devices using InAs  
13  
14 nanowires as building blocks.<sup>2</sup> Due to their superb electronic properties and strong quantum  
15  
16 confinement effects, they are also highly suitable for a large range of other applications such as  
17  
18 transistors,<sup>3-7</sup> p-n junctions,<sup>4,8</sup> high-performance nanoelectronics,<sup>9,10</sup> logical elements,<sup>11</sup> single  
19  
20 electron circuits,<sup>2,12-15</sup> spintronic<sup>16</sup> and quantum electronic devices.<sup>2,16-20</sup>  
21  
22  
23

24  
25 NWs have significant advantages over thin films and bulk materials due to their small  
26  
27 dimensions: diameter of up to few hundred nanometers and length of several microns.<sup>21,22</sup> They  
28  
29 can be integrated on a large variety of substrates such as silicon or organic polymers,<sup>23-25</sup> because  
30  
31 their small contact area with the substrate confines the strain relaxation-formed dislocations to  
32  
33 the NW/substrate interface. This means great flexibility in device design, potential for low cost  
34  
35 fabrication and seamless integration with silicon industrial platform. The small dimensions can  
36  
37 also result in quantum confinement of carriers.<sup>26</sup> Geometry of the NWs is especially beneficial  
38  
39 for photovoltaic and detector applications due to their low reflectivity and enhanced  
40  
41 absorption.<sup>27-29</sup> It also provides an efficient path for charge separation and carrier extraction  
42  
43 crucial for robust operation of photovoltaic devices.  
44  
45  
46  
47

48  
49 The main challenge in producing high-performance InAs NWs-based optoelectronic and  
50  
51 photonic devices is that good optical properties are hard to achieve. This is caused by poor  
52  
53 material quality and high levels of surface states emission due to large surface-to-volume ratio of  
54  
55 NWs and defect states near surfaces.<sup>30</sup> While high surface electron density of InAs is a desirable  
56  
57  
58  
59  
60

1  
2  
3 characteristic for electronic devices due to ease of ohmic contact formation, it hinders the optical  
4 performance. Due to this roadblock, most studies so far focused on electrical properties of the  
5 InAs nanowires<sup>7,31,32</sup> and fabrication of electronic and quantum devices. Only recently some low  
6 temperature optical studies have been reported,<sup>26,33-35</sup> but the signal quality is low due to high  
7 numbers of defects and impurities.  
8  
9

10  
11 We have identified two key factors required to achieve strong emission from the nanowires and  
12 hence obtain high quality devices: improved material quality and suppression of surface states.  
13 High-quality InAs nanowires have been demonstrated by using Au catalyst particles,<sup>2,9,33,34,36,37-41</sup>  
14 but these are not compatible with complementary metal-oxide-semiconductor (CMOS) industrial  
15 standards. Therefore, a self-catalysed growth method is more suitable. However, it requires fine  
16 levels of control in order to successfully produce high quality material. This level of precision  
17 can be achieved using molecular beam epitaxy (MBE), where the high-vacuum environment also  
18 helps in reducing incorporation of impurities. Elimination of surface states can be achieved by  
19 passivation of the NWs using a thin coating layer of other, less susceptible material.  
20  
21  
22  
23  
24  
25  
26  
27  
28  
29  
30  
31  
32  
33  
34  
35  
36

37 In this work, we investigate the effects of using an ultra-thin InP capping layer on optical  
38 properties of the InAs NWs. For this purpose, two samples have been grown and analyzed: core-  
39 only InAs NWs and InAs/InP core/shell NWs. We demonstrate successful surface passivation  
40 and hence an up to ten-fold improvement in photoluminescence emission. Moreover, good  
41 temperature stability and high carrier confinement has been observed for both samples, which  
42 lead to strong emission even at room temperature. This work overcomes a major roadblock of  
43 poor optical properties from InAs NWs, and hence could potentially enable successful realization  
44 of InAs NW photonic and optoelectronic devices.  
45  
46  
47  
48  
49  
50  
51  
52  
53  
54  
55  
56  
57  
58  
59  
60

The nanowires have been grown by a solid-source Veeco Gen930 molecular beam epitaxy (MBE) system with solid In source and As<sub>4</sub> and P<sub>2</sub> cracker cells. The self-catalyzed InAs NWs were grown directly on p-type Si(111) substrate at an In flux, V/III ratio, temperature and growth duration of 4.78×10<sup>-8</sup> Torr, 288, 450°C and 1 hour, respectively. The InP shell was grown at an In flux, V/III ratio, temperature and growth duration of 4.78×10<sup>-8</sup> Torr, 60, 400°C and 10 minutes, respectively.

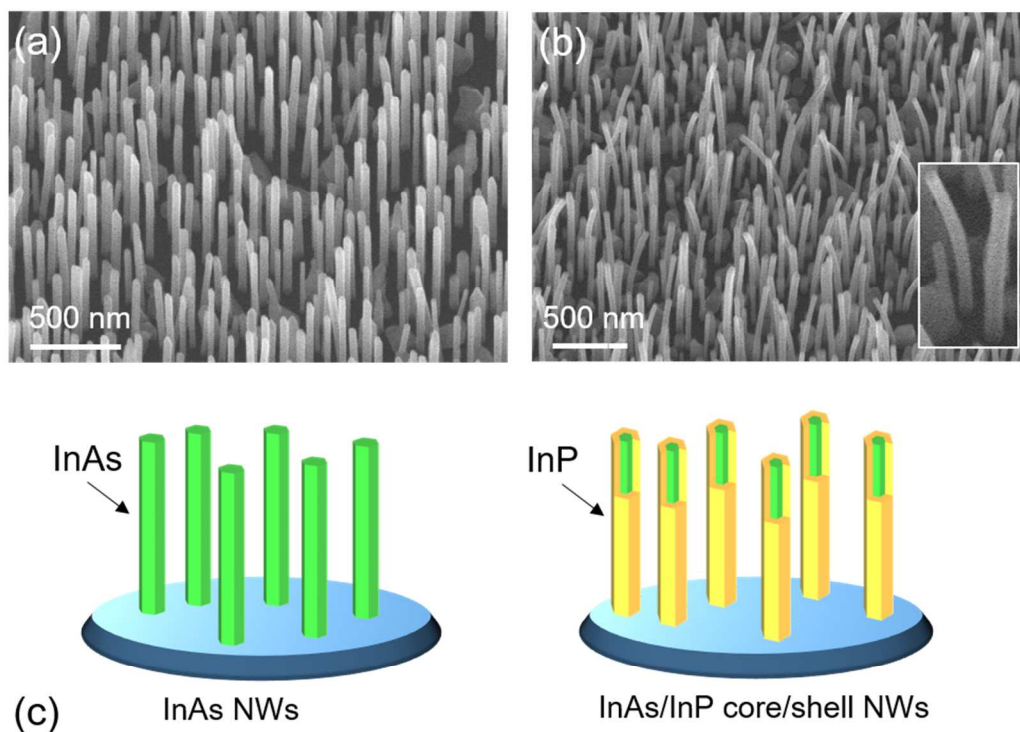


**Figure 1.** SEM images (tilt angle 25°) of (a) InAs core-only NWs and (b) InAs/InP core/shell NWs grown on Si(111) substrates via a self-catalyzed MBE growth method. The inset in (b) shows a high magnification image of single InAs/InP nanowires. (c) Illustration of InAs core-only NWs and InAs/InP core/shell NWs.

Figures 1a and 1b show tilted view (25°) of InAs core-only NWs and InAs/InP core/shell NWs, respectively. The nanowires have been grown vertically on the silicon substrate. The schematics of the NWs are shown in Fig. 1c. They are of good overall quality and are uniform in diameter,

1  
2  
3 density and length. For both samples the NWs are about 500 nm long with diameters of 55-60  
4 nm, 3-5 nm of which in InAs/InP nanowires account for the shell (shell thickness determined by  
5 TEM, Fig. 2(a)). There is a noticeable difference in the shape of the nanowires. While the core-  
6 only NWs are perfectly straight, the core/shell ones are visibly bent, which is caused by stress  
7 induced on the core of the nanowire by the shell.  
8  
9  
10  
11  
12  
13  
14  
15  
16  
17  
18  
19  
20  
21  
22  
23  
24  
25  
26  
27  
28  
29  
30  
31  
32  
33  
34  
35  
36  
37  
38  
39  
40  
41  
42  
43  
44  
45  
46  
47  
48  
49  
50  
51  
52  
53  
54  
55  
56  
57  
58  
59  
60

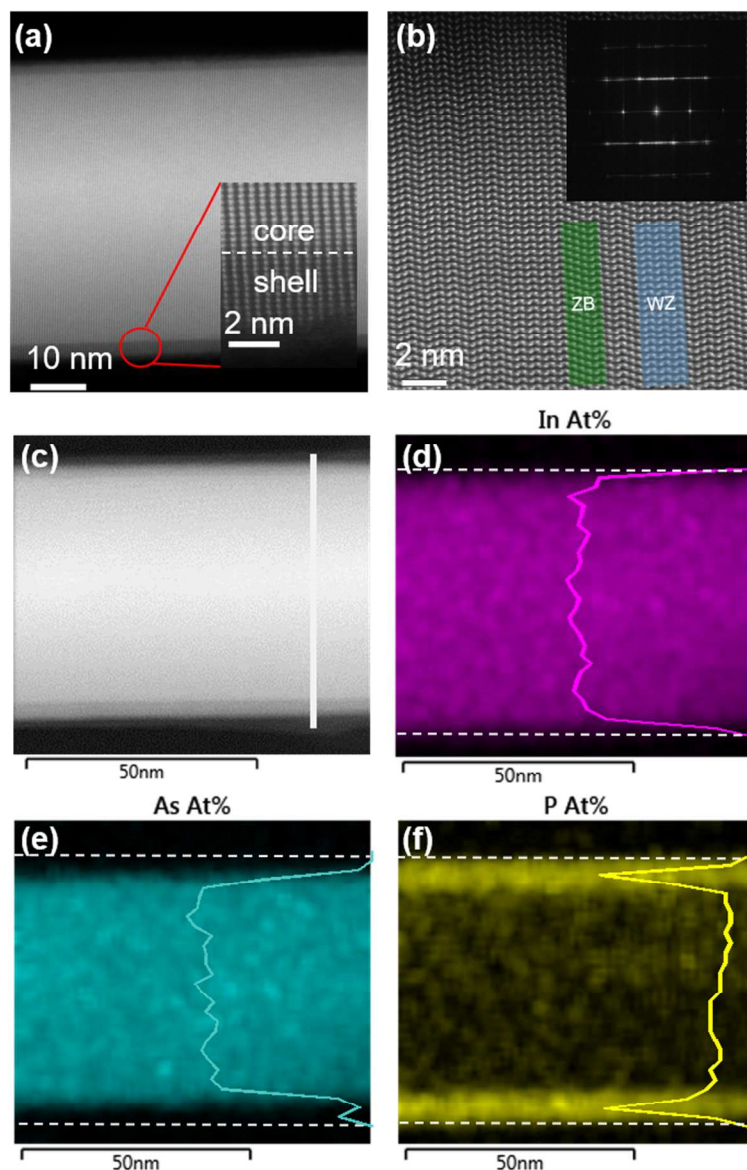


**Figure 2.** (a)  $\langle 112 \rangle$  ADF-STEM image of a middle section of one of the InAs/InP NWs clearly showing the core and shell parts of the structure. (b)  $\langle 110 \rangle$  ADF-STEM image of a middle

1  
2  
3 section of one of the InAs/InP NWs showing polytypic structure of the nanowires with  
4 highlighted examples of wurtzite (blue) and zinc-blende (green) crystal phases. The inset shows  
5 the selective area electron diffraction pattern taken for one of the nanowires confirming that both  
6 wurtzite (WZ) and zinc-blende (ZB) phases are present. Analysis of the composition of the  
7 InAs/InP NWs with EDX. (c) Middle section of a NW with highlighted (d) In, (e) As and (f) P  
8 elemental distribution as a percentage of all the elements in the nanowire (at%). EDX line profile  
9 taken along the white line indicated in (c) corresponding to the In, As and P have also been  
10 plotted in (d), (e) and (f), respectively.  
11  
12

13  
14 The ADF-STEM images of the InAs/InP sample have been taken using a doubly aberration  
15 corrected ARM 200 microscope. Figure 2a confirms presence of a thin, around 3 nm thick shell  
16 with different composition than the core. No defects have been observed at the interface between  
17 the InAs core and the InP shell. The ADF-STEM image in Figure 2b shows atomic stacking  
18 within the InAs/InP nanowire. A polytypic structure of the nanowires is clearly revealed with  
19 highlighted examples of WZ (blue) and ZB (green) crystal phases. Both phases are present and it  
20 has also been confirmed by the selective area electron diffraction pattern (Figure 2b inset). The  
21 composition switches between the two phases depending on fluctuations of growth temperature  
22 and flux ratios. Further work on the growth conditions is required in order to fine tune these  
23 parameters and obtain pure-phase InAs NWs.  
24  
25  
26  
27  
28  
29  
30  
31  
32  
33  
34  
35  
36  
37  
38

39 Figure 2c-f shows the results of composition analysis of the InAs/InP NWs performed with  
40 energy-dispersive x-ray spectroscopy (EDS). Fragment of a middle section of a nanowire, shown  
41 in Figure 2c, has been analyzed and showed uniform distribution of indium throughout the  
42 sample (Figure 2d) and arsenic (Figure 2e) within the core. Figure 2f shows high phosphorus  
43 content within the thin shell of the nanowire. However, the InAs/InP interface is not abrupt and  
44 some intermixing of P with As occurs in the InAs atomic layers close to the shell. The line plots  
45 in Figure 2d-f show concentrations of In, As and P atoms along the cross section of a middle part  
46  
47  
48  
49  
50  
51  
52  
53  
54  
55  
56  
57  
58  
59  
60



of the NW indicated with the line in Figure 2c. This confirms the composition of the core as InAs and the shell as InP.

A mid-IR PL setup has been used to analyze the photoluminescence properties of both samples. A 532 nm laser has been used to illuminate the samples and a liquid nitrogen cooled InSb detector to record the photoluminescence of the samples. In order to ensure that the collected signal originated from the nanowires, prior to the measurements they have been mechanically removed from the as-grown sample (via ultrasonication) and placed on a clean piece of silicon substrate. During the deposition process, certain steps were taken to make sure the densities are comparable. The samples were placed in a closed-cycle liquid helium cooled cryostat kept under vacuum. The measurements have been taken at a range of temperatures between 10 and 300 K. For power-dependent measurements laser powers between 50 and 600 mW have been used, where the power delivered to the sample is half of the laser output. For temperature-dependent measurements laser power of 600 mW (300 mW at the sample) has been used.

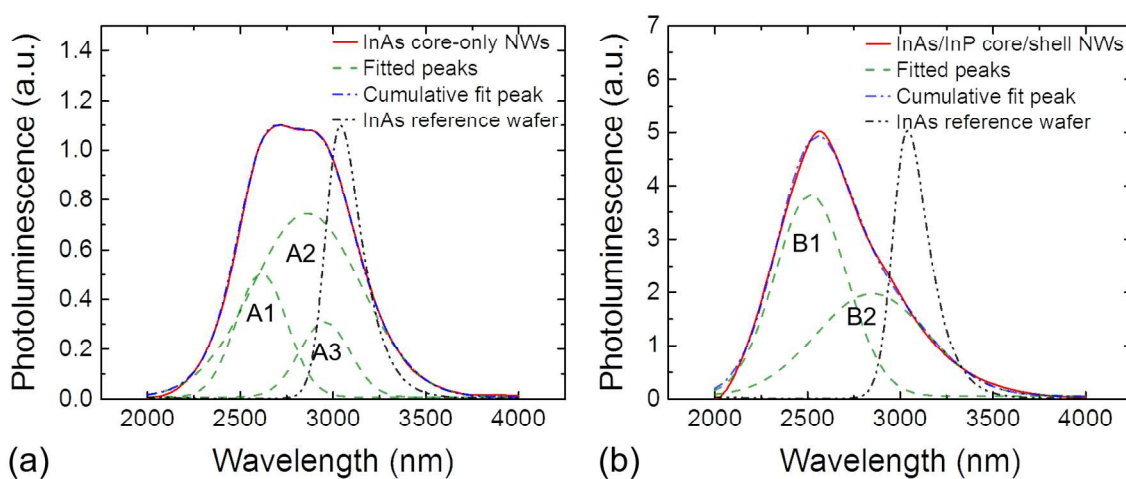


**Figure 3.** PL spectra taken at 10K for (a) the InAs core-only and (b) the InAs/InP core/shell nanowires with InAs wafer emission as reference. Measured signal (red), fitted Gaussian peaks (green), sum of the fitted peaks (blue) and normalized InAs wafer reference (black) have been plotted.

1  
2  
3  
4  
5  
6 Figure 3a shows PL spectrum of the InAs nanowires taken at 10 K. The spectrum can be  
7  
8 resolved into three peaks, A1 centered around 2607 nm (475.6 meV), A2 at 2835 nm (437.3  
9  
10 meV) and A3 at 2932 nm (422.9 meV). Figure 4b shows that only two peaks are present in the  
11  
12 PL spectrum of the InAs/InP nanowires, B1 at 2524 nm (491.2 meV) and B2 at 2833 nm (437.6  
13  
14 meV). All of the peaks observed in Figures 3a and 3b are blue-shifted from the bulk InAs  
15  
16 emission (around 3000 nm, 415 meV from literature;<sup>43</sup> 3026 nm, 409.7 meV from measurement  
17  
18 of InAs (ZB) wafer, reference peaks in Figure 3a and 3b). This is most probably caused by size-  
19  
20 induced quantization effects or Burstein-Moss (band-filling) effect commonly observed for  
21  
22 nanowires.<sup>44</sup> There is also a slight blue shift of the InAs/InP PL peaks compared to core-only  
23  
24 InAs due to strain induced by the InP cladding.<sup>45,46</sup> The energy difference between peaks B1 and  
25  
26 B2 is 53.6 meV, which is very close to the theoretically predicted difference between bandgaps  
27  
28 of wurtzite and zinc blende phases in InAs bulk by Zanolli et al.<sup>47</sup> The energy difference between  
29  
30 peaks A1 and A3 can be calculated to equal 52.7 meV, also very close to the theoretical  
31  
32 prediction. These observations lead us to believe that peaks A1 and B1 arise from the WZ  
33  
34 segments of the nanowires, while peaks A3 and B2 arise from the ZB segments. Due to small  
35  
36 diameter of the NWs and high surface electron density in InAs, surface effects dominate  
37  
38 recombination processes in InAs NWs. The InP shell passivates the surface and hence suppresses  
39  
40 the surface emission in favor of emission from the NW core. Hence peak A2, which is dominant  
41  
42 in intensity for the InAs core-only sample, can be attributed to surface states related emission  
43  
44 while an analogous peak is not present in the passivated InAs/InP sample.  
45  
46  
47  
48  
49  
50  
51  
52  
53  
54  
55  
56  
57  
58  
59  
60

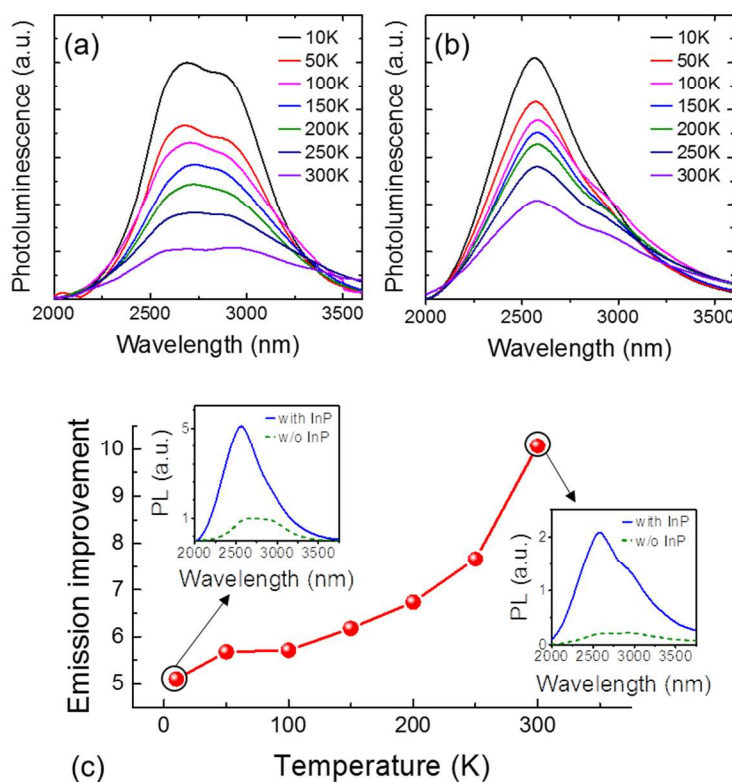


**Figure 4.** PL spectra taken at temperatures between 10 and 300 K for (a) the InAs core-only and (b) the InAs/InP core/shell nanowires. (c) Emission improvement of the InAs/InP NWs over InAs NWs, the insets show PL emission for the two samples at 10 and 300 K.

Figure 4 shows the PL spectra taken for both samples at temperatures between 10 and 300 K. The general shape of the spectra does not change with temperature for the InAs/InP sample (Figure 4b) and the intensity drops with increasing temperature as expected. For the InAs sample (Figure 4a) the relative intensities of the peaks in the spectra change at sample temperatures of 200 K and above. This is due to increased surface states emission relative to the nanowires emission as the surface related processes are more significant at higher temperatures. Strong emission can be observed all the way up to room temperature (300 K), where the intensities of InAs and InAs/InP samples are about 20% and 40% of that at 10 K, respectively. Achieving strong room temperature emission from these nanowires confirms high quality of the material and indicates that it is possible to fabricate InAs NWs-based photonic devices capable of

1  
2  
3 operating at room conditions in near future. Figure 4c shows the emission improvement of the  
4 InP-capped NWs compared to the InAs core-only NWs calculated as a ratio of the maximum  
5 peak intensities of the two samples. The ratio increases with the temperature as the InAs NWs  
6 are more strongly affected by the thermal effects due to their unpassivated surfaces, which once  
7 again confirms the effectiveness of the InP capping layer. At 10 K the overall strength of PL  
8 emission from the InAs/InP core/shell NWs is about five times stronger, while at room  
9 temperature we observe a ten-fold improvement.

10  
11  
12  
13  
14  
15  
16  
17  
18  
19  
20 Figure 5 presents results for integrated PL values as function of excitation power and  
21 temperature. In Figure 5a a typical trend can be observed for the InAs/InP NWs sample where  
22 the integrated PL values rise quickly with increasing power at low powers (up to around 100  
23 mW), and then starts to saturate at higher powers. The shapes of these plots do not change  
24 between different sample temperatures, only the overall strength drops as expected based on  
25 temperature-dependent PL measurements. For the InAs core-only sample the general trends of  
26 the plots are similar to those for InAs/InP, however the saturation point moves towards higher  
27 excitation powers as the temperature is increased. These results show that thermally excited  
28 recombination processes become more severe as the sample warms up and suggest that the  
29 surface states are responsible. Comparing the plots for the two samples it can be observed that  
30 the improvement achieved by addition of InP passivation layer is substantial in terms of PL  
31 output of the samples.  
32  
33  
34  
35  
36  
37  
38  
39  
40  
41  
42  
43  
44  
45  
46  
47  
48  
49  
50  
51  
52  
53  
54  
55  
56  
57  
58  
59  
60

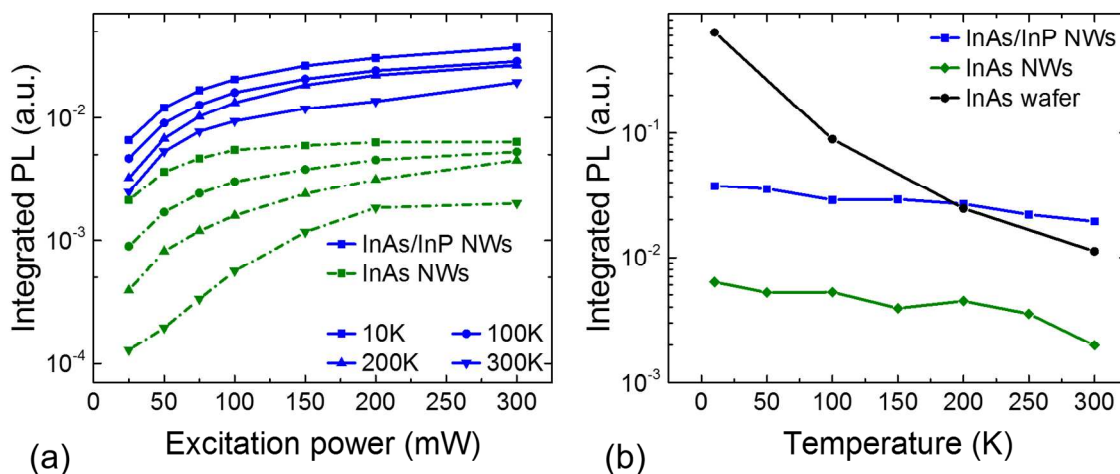


**Figure 5.** Integrated PL as a function of (a) excitation power for a range of temperatures between 10 and 300 K and (b) sample temperature for InAs/InP nanowires (blue), InAs core-only nanowires (green) and InAs wafer (black).

Figure 5b shows how the integrated PL values behave in terms of sample temperature. A usual trend is observed for the InAs wafer, where the integrated PL strength drops rapidly as the temperature is increased by more than order of magnitude between 10 K and room temperature. Both nanowire samples however show remarkable stability across the whole range of temperatures. The integrated PL intensity for the InAs/InP (InAs) sample between 10 and 300 K drops only by a factor of 2 (3). We attribute this behavior to very high carrier confinement within the nanowires. Because of small dimensions of each of the nanowires and small contact area with the substrate, the thermally excited carriers cannot easily escape and then non-radiatively recombine as it happens in bulk materials. The fact that similar trends are observed for both nanowire samples indicate that the effects of confinement are much stronger than any negative influence of surface states. It is also interesting to notice that at temperatures above 200 K the integrated PL of InAs/InP NW sample is higher than that of the InAs wafer. This could be explained by the geometry of the wafer (bulk material) and that it is not passivated.

1  
2  
3 In conclusion, the effects of InP capping on the optical emission of InAs NWs have been  
4 investigated. Effective surface passivation resulted in up to ten-fold improvement of  
5 photoluminescence emission from the nanowires when compared to the core-only sample. We  
6 presented the first demonstration of room-temperature PL emission from InAs nanowires.  
7  
8 Moreover, high carrier confinement within these nanowires can be an important advantage in  
9 design of novel electronic and quantum devices or lead to new observations of nanoscale  
10 physical phenomena. The results presented here could a high impact on the development of InAs  
11 NWs optoelectronic materials and devices.  
12  
13  
14  
15  
16  
17  
18  
19  
20  
21

## 22 **AUTHOR INFORMATION**

### 23 **Corresponding Author**

24  
25  
26  
27  
28 \* [pamela.jurczak.10@ucl.ac.uk](mailto:pamela.jurczak.10@ucl.ac.uk), \* [yunyan.zhang.11@ucl.ac.uk](mailto:yunyan.zhang.11@ucl.ac.uk), \* [jiang.wu@ucl.ac.uk](mailto:jiang.wu@ucl.ac.uk)  
29  
30

### 31 **Author Contributions**

32  
33  
34 The manuscript was written through contributions of all authors. All authors have given approval  
35 to the final version of the manuscript. <sup>□</sup>These authors contributed equally.  
36  
37  
38

### 39 **Notes**

40  
41  
42 The authors declare no competing financial interests.  
43  
44

## 45 **ACKNOWLEDGMENT**

46  
47  
48 The authors acknowledge financial support from UK EPSRC under Grant No. EP/P000886/1 and  
49 Leverhulme Trust.  
50  
51

## 52 **REFERENCES**

53  
54  
55  
56 [1] – Milnes, A.G.; Polyakov, A.Y. *Mat. Sci. Eng. B* **1993**, 18, 237-259  
57  
58  
59  
60

1  
2  
3 [2] – Fasth, C.; Fuhrer, A.; Samuelson, L.; Golovach, V.N.; Loss, D. *Phys. Rev. Lett.* **2007**, 98,  
4  
5 266801  
6

7  
8 [3] – Goldberger, J.; Sirbuly, D.J.; Law, M.; Yang, P. *J. Phys. Chem. B* **2004**, 109, 9-14  
9

10  
11 [4] – Greytak, A.B.; Lauhon, L.J.; Gudiksen, M.S.; Lieber, C.M. *Appl. Phys. Lett.* **2004**, 84,  
12  
13 21  
14

15  
16 [5] – Cui, Y.; Lieber, C.M. *Science* **2001**, 291, 5505, 851-853  
17

18  
19 [6] – Ghalamestani, S.G.; Johansson, S.; Borg, B.M.; Lind, E.; Dick, K.A.; Wernersson, L.E.  
20  
21 *Nanotechnology* **2012**, 23, 015302  
22

23  
24 [7] – Tanaka, T.; Tomioka, K.; Hara, S.; Motohisa, J.; Sano, E.; Fukui, T. *Appl. Phys. Express*  
25  
26 **2010**, 3, 025003  
27

28  
29 [8] – Haraguchi, K.; Katsuyama, T.; Hiruma, K.; Ogawa, K. *Appl. Phys. Lett.* **1991**, 60,  
30  
31 106556  
32

33  
34 [9] – Thelander, C.; Bjork, M.T.; Larsson, M.W.; Hansen, A.E.; Wallenberg, L.R.; Samuelson,  
35  
36 L. *Solid State Comm.* **2004**, 131, 573-579  
37

38  
39 [10] – Jiang, X.; Xiong, Q.; Nam, S.; Qian, F.; Li, Y.; Lieber, C.M. *Nano Lett.* **2007**, 7, 3214-  
40  
41 3218  
42

43  
44 [11] – Huang, Y.; Duan, X.; Cui, Y.; Lauhon, L.J.; Kim, K.H.; Lieber, C.M. *Science* **2001**,  
45  
46 294, 5545  
47

48  
49 [12] – Zhong, Z.; Fang, Y.; Lu, W.; Lieber, C.M. *Nano Lett.* **2005**, 5, 1143-1146  
50

51  
52 [13] – Thelander, C.; Martensson, T.; Bjork, M.T.; Ohlsson, B.J.; Larsson, M.W.; Wallenberg,  
53  
54 L.R.; Samuelson, L. *Appl. Phys. Lett.* **2003**, 83, 10  
55  
56  
57  
58  
59  
60

1  
2  
3 [14] – Bjork, M.T.; Thelander, C.; Hansen, A.E.; Jensen, L.E.; Larsson, M.W.; Wallenberg,  
4 L.R.; Samuelson, L. *Nano Lett.* **2004**, 4, 1621-1625  
5  
6

7  
8 [15] – De Franceschi, S.; van Dam, J.A.; Bakkers, E.P.A.M.; Feiner, L.F.; Gurevich, L.;  
9 Kouwenhoven, L.P. *Appl. Phys. Lett.* **2003**, 83, 2  
10  
11

12  
13 [16] – Bjork, M.T.; Fuhrer, A.; Hansen, A.E.; Larsson, M.W.; Froberg, L.E.; Samuelson, L.  
14 *Phys. Rev. B* **2005**, 72, 201307  
15  
16

17  
18 [17] – Kang, J.H.; Ronen, Y.; Cohen, Y.; Convertino, D.; Rossi, A.; Coletti, C.; Heun, S.;  
19 Sorba, L.; Kacman, P.; Shtrikman, H. *Semicond. Sci. Technol.* **2016**, 31, 115005  
20  
21  
22

23  
24 [18] – Loss, D.; DiVincenzo, D.P. *Phys. Rev. A* **1998**, 57,120  
25  
26

27 [19] – Burkard, G.; Loss, D.; DiVincenzo, D.P. *Phys. Rev. B* **1999**, 59, 2070  
28  
29

30 [20] – Lu, Wei; Lieber, C.M. *J. Phys. D Appl. Phys.* **2006**, 39, R387  
31  
32

33 [21] – Hu, Y.; Churchill, H.O.H.; Reilly, D.J.; Xiang, J.; Lieber, C.M.; Marcus, C.M. *Nature*  
34 *Nanotechnology* **2007**, 2, 622-625  
35  
36

37 [22] – Zhang, Y.; Wu, J.; Aagesen, M.; Liu, H. *J. Phys. D Appl. Phys.* **2015**, 48, 463001  
38  
39

40 [23] – Zhang, Y.; Aagesen, M.; Holm, J.V.; Jorgensen, H.I.; Wu, J.; Liu, H. *Nano Lett.* **2013**,  
41 13, 3897-3902  
42  
43  
44

45 [24] – Matteini, F.; Tutuncuoglu, G.; Ruffer, D.; Alarcon-Llado, E.; Fontcuberta i Morral, A. *J.*  
46 *Crys. Growth* **2014**, 404, 246-255  
47  
48  
49

50 [25] – Klein, L.; Mastrogiovanni, D.; Wan, A.; Garfunkel, E. *InTech* **2011**, Chapter 16  
51  
52

53 [26] – Koblmuller, G.; Vizbaras, K.; Hertenberger, S.; Bolte, S.; Rudolph, D.; Becker, J.;  
54 Doblinger, M.; Amann, M.C.; Finley, J.J.; Abstreiter, G. *Appl. Phys. Lett.* **2012**, 101, 5  
55  
56  
57  
58  
59  
60



1  
2  
3 [27] – Yablonovitch, E.; Cody, G.D. *IEEE T. Electron. Dev.* **1982**, 29, 300-305  
4

5  
6 [28] – Krogstrup, P.; Jorgensen, H.I.; Heiss, M.; Demichel, O.; Holm, J.V.; Aagesen, M.;  
7  
8 Nygard, J.; Fontcuberta i Morral, A. *Nature Photonics* **2013**, 7, 306-310  
9

10  
11 [29] – Yablonovitch, E. *J.Opt. Soc. Am.* **1982**, 72, 899-907  
12

13  
14 [30] – Lu, A.; Zhao, C.; Wu, J. *J. Nanosc. Nanotech.* **2016**, 16, 8146-8149  
15

16  
17 [31] – Ford, A.C.; Ho, J.C.; Chueh, Y.L.; Tseng, Y.C.; Fan, Z.; Guo, J.; Bokor, J.; Javey, A.  
18  
19 *Nano Lett.* **2009**, 9, 360-365  
20

21  
22 [32] – Wei, W.; Bao, X.Y.; Soci, C.; Ding, Y.; Wang, Z.L.; Wang, D. *Nano Lett.* **2009**, 9,  
23  
24 2926-2934  
25

26  
27 [33] – Sun, M.H.; Leong, E.S.P.; Chin, A.H.; Ning, C.Z.; Cirilin, G.E.; Samsonenko, Y.B.;  
28  
29 Dubrovskii, V.G.; Chuang, L.; Chang-Hasnain, C. *Nanotechnology* **2010**, 21, 33  
30

31  
32 [34] – Rota, M.B.; Ameruddin, A.S.; Fonseka, H.A.; Gao, Q.; Mura, F.; Polimeni, A.;  
33  
34 Miriametro, A.; Tan, H.H.; Jagadish, C.; Capizzi, M. *Nano Lett.* **2016**, 16, 5197-5203  
35

36  
37 [35] – Hormann, N.G.; Zardo, I.; Hertenberger, S.; Funk, S.; Bolte, S.; Doblinger, M.;  
38  
39 Koblmuller, G.; Abstreiter, G. *Phys. Rev. B* **2011**, 84, 155301  
40

41  
42 [36] – Dubrovskii, V.G.; Sibirev, N.V.; Berdnikov, Y.; Gomes, U.P.; Ercolani, D.; Zannier, V.;  
43  
44 Sorba, L. *Nanotechnology* **2016**, 27, 375602  
45

46  
47 [37] – Dick, K.A.; Thelander, C.; Samuelson, L.; Caroff, P. *Nano Lett.* **2010**, 10, 3494-3499  
48

49  
50 [38] – Caroff, P.; Dick, K.A.; Johansson, J.; Messing, M.E.; Deppert, K.; Samuelson, L. *Nature*  
51  
52 *Nanotechnology* **2009**, 4, 50-55  
53  
54  
55  
56  
57  
58  
59  
60

1  
2  
3 [39] – Chuang, L.C.; Moewe, M.; Chase, C.; Kobayashi, N.P.; Chang-Hasnain, C.; Crankshaw,  
4  
5  
6 S. *Appl. Phys. Lett.* **2007**, 90, 4

7  
8 [40] – Roest, A.L.; Verheijen, M.A.; Wunnicke, O.; Serafin, S.; Wondergem, H.; Bakkers,  
9  
10  
11 E.P.A.M. *Nanotechnology* **2006**, 17, S271

12  
13 [41] – Tchernycheva, M.; Travers, L.; Patriarche, G.; Glas, F.; Harmand, J.C.; Cirlin, G.E.;  
14  
15  
16 Dubrovskii, V.G. *J. Appl. Phys.* **2007**, 102, 9

17  
18 [42] – Lin, H.M.; Chen, Y.L.; Yang, J.; Liu, Y.C.; Yin, K.M.; Kai, J.J.; Chen, F.R.; Chen,  
19  
20  
21 L.C.; Chen, Y.F.; Chen, C.C. *Nano Lett.* **2003**, 3, 537-541

22  
23 [43] – InAs band structure and carrier concentration, IOFFE institute, accessed on 3<sup>rd</sup> February  
24  
25  
26 2017, <http://www.ioffe.ru/SVA/NSM/Semicond/InAs/bandstr.html>

27  
28 [44] – Yan, Y.; Liao, Z.M.; Bie, Y.Q.; Wu, H.C.; Zhou, Y.B. *Appl. Phys. Lett.* **2011**, 99, 10

29  
30 [45] – Shiri, D.; Kong, Y.; Buin, A.; Anantram, M.P. *Appl. Phys. Lett.* **2008**, 93, 7

31  
32 [46] – Wei, B.; Zheng, K.; Ji, Y.; Zhang, Y.; Zhang, Z.; Han, X. *Nano Lett.* **2012**, 12, 4595-  
33  
34  
35 4599

36  
37 [47] – Zanolli, Z.; Fuchs, F.; Furthmuller, J.; von Barth, U.; Bechstedt, F. *Phys. Rev. B* **2007**,  
38  
39  
40 75, 245121